Accepted Manuscript

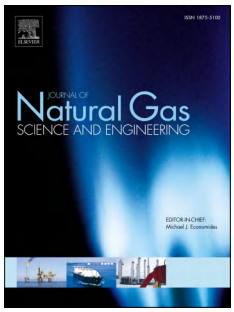

High injection rate stimulation for improving the fracture complexity in tight-oil sandstone reservoirs

Chuang Liu, Fang Shi, YongPing Zhang, YuGuang Zhang, DaWei Deng, XiaoLong Wang, He Liu, HengAn Wu

PII: S1875-5100(17)30113-0

DOI: 10.1016/j.jngse.2017.03.007

Reference: JNGSE 2105

To appear in: *Journal of Natural Gas Science and Engineering*

Received Date: 26 October 2016

Revised Date: 19 January 2017

Accepted Date: 3 March 2017

Please cite this article as: Liu, C., Shi, F., Zhang, Y., Zhang, Y., Deng, D., Wang, X., Liu, H., Wu, H., High injection rate stimulation for improving the fracture complexity in tight-oil sandstone reservoirs, *Journal of Natural Gas Science & Engineering* (2017), doi: 10.1016/j.jngse.2017.03.007.

High injection rate stimulation for improving the fracture complexity in tight-oil sandstone reservoirs

Chuang Liu[a], Fang Shi[a], YongPing Zhang[b], YuGuang Zhang[b], DaWei Deng[b], XiaoLong Wang[a], He Liu[c] and HengAn Wu[a,*]

[a] CAS Key Laboratory of Mechanical Behavior and Design of Materials, Department of Modern Mechanics, University of Science and Technology of China, Hefei, Anhui 230027 China

[b] PetroChina Daqing Oil Field Limited Company, Daqing, Heilongjiang 163454 China

[c] PetroChina Research Institute of Petroleum Exploration & Development, Beijing 100083 China

*Corresponding author, Tel/Fax: 0086-551-63601245, Email: wuha@ustc.edu.cn

Abstract: Successfully creating a large field fracture network is crucial for achieving economic production of tight-oil sandstone reservoirs. In this paper, the variations of in situ stress as well as the fracture network are studied based on a fully coupled flow and mechanics model. A high injection rate stimulation technique is extensively investigated as an effective method for improving the fracture complexity in single or multiple stages of horizontal well. Sensitivity studies are conducted for this stimulation method in improving the fracture complexity. The high injection rate stimulation cannot efficiently promote the fracture network area for ductile rocks. Initial in situ stress contrast plays an important role in the creation of fracture network. The fracture aperture as well as stress perturbation is controlled by the minimum in situ stress. The stress perturbation is accentuated in low permeability reservoirs, which is helpful to achieve a large field of fracture network. The area of new created

fracture network in sequential fracturing is increasing with the fractures due to the arising of mechanical interaction between fractures. The results presented in this paper can be used in hydraulic fracturing design in tight-oil sandstone reservoirs to promote productivity.

Keywords: sandstone reservoirs, fracture network, hydraulic fracturing, injection rate

1. Introduction

Hydraulic fracturing has been widely used in unconventional reservoir exploitation, such as shale-gas and oil reservoirs. Investigating the propagation of fluid-driven hydraulic fractures and fracture networks remains challenging work due to the complex coupling of multi-physics and different scales of the problem (Weng, 2015). Significant progress has been made in modeling hydraulic fractures by analytical and numerical methods in recent years. The proppant transport and settling in hydraulic fractures were theoretically investigated by Dontsov and Peirce (2014, 2015). The cohesive element method has been used to simulate single and multiple fracture propagation (Chen, 2012; Guo et al., 2015a; Wang et al., 2015). The extended finite element method (XFEM) has been proposed and developed to simulate hydraulic fractures propagation problems (Belytschko and Black, 1999; Dahi-Taleghani and Olson, 2011; Shi et al., 2016). This method allows fractures to propagate within elements; therefore, it is able to model arbitrary discontinuities independent of the meshes. Simulating fracture propagation in fluid-filled porous media based on XFEM was developed (Mohammadnejad and Andrade, 2016;

Mohammadnejad and Khoei, 2013a; Mohammadnejad and Khoei, 2013b). Wang (2015) and Wang et al. (2016) used an XFEM-based cohesive zone method to simulate nonplanar fracture propagation. Olson and Dahi-Taleghani (2009) developed a displacement discontinuity model (DDM) to simulate multiple fracture propagation in a reservoir containing pre-exiting natural fractures. The mechanical interaction between hydraulic and natural fractures during stimulation is neglected in the model. Zhang and Jeffrey (2014) built a fully coupled fracture interaction model based on a two-dimensional DDM method. The model incorporates reopening and slippage of natural fracture, and it is time-consuming to stimulate a large number of fractures. Kresse et al. (2013) developed a pseudo-3D DDM model to simulate complex fracture, using an analytical OpenT crossing model, and improve the calculation speed. Riahi and Damjanac (2013) used a 2D-DFN model to study the effect of the fracture connectivity on the induced hydraulic fracture network. However, the fluid can only flow along the predefined connected DFN paths. A comprehensive model to predict the fracture geometry and network for practical engineering application remains to be estimated.

The optimal design of hydraulic fracture treatments has been investigated by many researchers. Zhou et al. (2014) numerically investigated a low-efficient hydraulic fracturing operation in a tight gas reservoir in the North German Basin. They calculated a reasonable position for the perforation to avoid the full closure of the fracture at the perforation. Many earlier researchers focused on the influence of in situ stress perturbation on fracture extension and fracture spacing optimization

(Morrill and Miskimins, 2012; Roussel and Sharma, 2011a; Roussel and Sharma, 2011b; Soliman et al., 2010). Morrill and Miskimins (2012) investigated the sensitivity of the stress shadow on various reservoir properties. Roussel and Sharma (2011b) performed a study of fracture mechanical interaction to evaluate the trajectory of multiple consecutive transverse fractures in horizontal well completions. The fracture propagation direction of their model is determined by the in situ stress field created by previous fractures. Soliman et al. (2010) studied the Texas-two step technique and noted that fracture spacing should be designed to achieve isotropy of in situ stress. Liu et al. (2015) numerically simulated the connectivity of the fracture network created by the Texas-two step method and proposed a new method for fracture spacing optimization in the horizontal shale-gas well. The previous results focus on the mechanical interaction between fractures of a given fracture length. However, the variations of in situ stress as well as its connection with fracture network during fracture propagation have not been presented yet.

The reopening and slippage of existing natural fracture by hydraulic fracture will greatly enhance the flow conductivity of a natural fracture (Zhao et al., 2013). Olson and Taleghani (2009) found that low in situ stress anisotropy tends to improve the fracture complexity in naturally fractured reservoirs. Fu et al. (2013) built an explicitly coupled hydro-geomechanical model for simulating hydraulic fracturing in arbitrary discrete fracture networks. Their results demonstrate that the large field of the fracture network can be created in low in situ stress contrast reservoirs. Guo et al. (2015b) simulated a hydraulic fracture crossing a cemented natural fracture. The in

situ stress contrast was a key parameter that contains how a hydraulic fracture propagates across a natural fracture. In some Chinese oilfields, the formation in situ stress contrast is large, which suppresses the growth of a fracture network. The approach for decreasing in situ stress anisotropy and improving fracture complexity in these reservoirs remains challenging work.

In this paper, we use a fully coupled hydro-mechanical propagation model based on XFEM to investigate fracture propagation as well as fracture network problems. The initiation, propagation of nonplanar fractures in porous medium and variations of in situ stress during the stimulation process are numerically simulated. Low in situ stress contrast regions during fracture propagation are regarded as fracture network zones in this paper. The evolution of the fracture network created by single and multiple fractures during the stimulation process is numerically simulated. Using this model, we study the effect of a high injection rate stimulation method on improving the fracture complexity in single and multiple fracture treatments. Sensitivity analysis of a high injection rate method for improving the fracture complexity is presented.

2. Fracture propagation model

The model presented in this paper is based on a two-dimension plane strain assumption and utilizes the XFEM to calculate stress interference and simulate fracture propagation. The fluid flow inside the fracture is governed by the Lubrication equation. The hydraulic fracture model couples fluid flow and fracture deformation through an iterative scheme between fracture aperture along the fracture length and

fluid pressure. The truss model is used to calculate the impact of the stress shadow by the propped fractures. The fracture propagation path is determined by the maximum principle in situ compressive stress. A brief summary of the modeling approach is presented here. Further details can be found in Liu et al. (2016).

2.1 Governing equations

Hydraulic fracture propagation couples fluid flow and rock deformation. The flow patterns of the fluid within the fracture are shown in Fig. 1. The fluid is assumed to be incompressible with Newtonian rheology. The tangential flow within the fracture is governed by the lubrication equations (Batchelor, 1967).

$$\boldsymbol{q} = -\frac{w^3}{12\mu}\nabla p_f \tag{1}$$

where $\boldsymbol{q}$ is the fluid flux of the tangential flow, p_f is the fluid pressure inside the fracture, w is the fracture opening, and μ is the fluid viscosity. The fluid leak-off in reopened natural fractures is not considered in this paper. The rock matrix is assumed to be isotropic and homogeneous. We simulated the fluid leak-off in hydraulic fractures with the fluid leak-off equations

$$\begin{cases} q_t = c_t\left(p_f - p_t\right) \\ q_b = c_b\left(p_f - p_b\right) \end{cases} \tag{2}$$

where c_t and c_b define the fluid leak-off coefficients for the top and bottom surfaces of a fracture, respectively. p_t and p_b are pore pressures in the adjacent formation.

In fluid filled porous media, the equilibrium equation can be written as

$$\nabla \cdot (\boldsymbol{\sigma}' - p_w \boldsymbol{I}) + \boldsymbol{f} = 0 \tag{3}$$

where $\boldsymbol{\sigma}'$ and $\boldsymbol{f}$ are the effective stress and body force per unit volume, respectively; p_w is the porous pressure; and $\boldsymbol{I}$ is the unit matrix. The relationship between the velocity of seepage flow and gradient of porous pressure satisfies Darcy's law (Marino and Luthin, 1982).

$$\boldsymbol{v}_w = -\frac{1}{\phi g \rho_w} \boldsymbol{k} \cdot \left(p_w - \rho_w \boldsymbol{g} \right) \tag{4}$$

where $\boldsymbol{k}$ and $\boldsymbol{g}$ represent the hydraulic conductivity tensor component and gravity acceleration vector, respectively.

2.2 The extended finite element method

The XFEM was first introduced by Belytschko and Black (1999). It is an extension of the conventional finite element method based on the concept of the partition of unity proposed by Melenk and Babuska (1996), which allows local enrichment functions to be easily incorporated into a finite element approximation. The presence of discontinuities is ensured by the special enriched functions in conjunction with additional degrees of freedom. Using the XFEM, the evolving crack is simulated independent of the finite element mesh. The approximation for a displacement vector function u_i without near-tip asymptotic singularity can be written as

$$u_i = \sum_I N_I \left(\boldsymbol{X} \right) u_{iI} + \sum_J \phi_J \left(\boldsymbol{X} \right) a_{iJ} \tag{5}$$

where $N_I \left(\boldsymbol{X} \right)$ is the usual nodal shape function, u_{iI} is the usual nodal displacement vector, $\phi_J \left(\boldsymbol{X} \right)$ is the enriched shape function, and a_{iJ} is the enriched

degree of freedom.

2.3 The cohesive law

The fracture propagation analysis is governed by cohesive traction-separation constitutive behavior. The traction-separation model assumes linear elastic behavior followed by the initiation and evolution of damage. The elastic behavior is written in terms of an elastic constitutive matrix that relates the normal and shear stresses to the normal and shear separations of a cracked element. Damage modeling simulates the degradation and eventual failure of an enriched element. The failure mechanism consists of the following two ingredients: a damage initiation criterion and evolution law. Damage initiation refers to the beginning of degradation of the cohesive response at an enriched element. The process of degradation begins when the stresses or the strains satisfy specified crack initiation criteria. The maximum principal stress criterion is used in this paper and it can be represented as

$$\left\{\frac{\langle \sigma_{max} \rangle}{\sigma_{max}^{0}}\right\} = 1 \tag{6}$$

where σ_{max} and σ_{max}^{0} represent the maximum principal stress and maximum allowable principal stress, respectively. The symbol $\langle\ \rangle$ signifies that a purely compressive stress state does not initiate damage.

The damage evolution law describes the rate at which the cohesive stiffness is degraded once the corresponding initiation criterion is reached. A scalar damage variable, D, represents the average overall damage. It initially has a value of 0. If damage evolution is modeled, D monotonically evolves from 0 to 1 upon further loading after the initiation of damage. The stress components are affected by the

damage according to

$$\boldsymbol{t} = \begin{cases} (1-D)\bar{\boldsymbol{t}} & \text{damage initiated} \\ \bar{\boldsymbol{t}} & \text{no damage occurs} \end{cases} \tag{7}$$

where $\bar{\boldsymbol{t}}$ are stress components predicted by the linear elastic traction-separation behavior for the current separations without damage.

3. Numerical results and discussion

All simulations presented in this paper were conducted by ABAQUS. To simulate a large formation and guarantee solution convergence, coarse and refined elements are used in the far and near fields of the fractures, respectively. The shape of the elements is rectangular. Different sizes of elements are connected using the TIE constraint. The Newton-Raphson iterative method is used to solve the coupled system of nonlinear equations. The input parameters used in this paper originated from a Chinese oilfield. The parameters were selected within the range of the field data.

3.1 Model verification

A model verification is presented through comparing surface pressure. A hydraulic fracturing process of a horizontal well in a Chinese oilfield is simulated. The injection rate is 4.5 m^3/min with the period of 280 min. The matrix permeability is 0.01 mD with the porosity of 0.064. The elastic modulus and Poisson's ratio are 46 GPa and 0.2, respectively. The horizontal in-situ stresses are 50 MPa and 61 MPa. Fig.2 shows the comparison of surface pressure from the measured pressure and the simulated one during the operation. The two curves match well during the fracturing process. The

verification of the model is approved. The manuscript was revised accordingly.

3.2 Results of single fracture treatments

3.2.1 Variations of in situ stress contrast during fracture propagation

The extension of a fracture in the rock causes changing in situ stress in its neighborhood, which then affects the initiation and propagation of natural fractures. The analytical solution of stress interference has been investigated by Sneddon and Elliott (1946). The analytical solution presents changing of in situ stress with a given net pressure and fracture length. However, this approach relies on the simplification of the problem with respect to the fracture opening profile. In this paper, the variation of in situ stress during fracture propagation is investigated using a fully coupled hydro-mechanical fracture extension model. The analysis is simplified to be two-dimensional as we assume that the fracture height is sufficiently large. The injection rate is 5 m^3/min. The other parameters are listed in Table 1. Due to the symmetry of geometry, material and load, only half of the model is considered. The variation of in situ stress contrast with the fracture length is demonstrated in Fig. 3. It is shown that the in situ stress contrast decreases in the vicinity of the fracture due to the increased minimum normal stress induced by the opened fracture. The in situ stress contrast along the horizontal well increases with the fracture length.

The reopening and slippage of existing natural fracture by hydraulic fracturing will greatly enhance the flow conductivity of natural fracture (Zhao et al., 2013). The in situ stress contrast is not a constant during hydraulic fracture propagation, as

demonstrated above. A hydraulic fracture propagating in a region of low stress contrast is likely to create a larger network of interconnected fractures (Fu et al., 2013; Olson and Taleghani, 2009). During the fracturing process, the fluid is leak-off from a hydraulic fracture and will reopen cemented natural fractures in a zone where the stress contrast is under a critical value. Numerical simulation of complex fracture networks is still a challenge work. The in situ stress contrast can be regarded as an indicator of the fracture network in a region. It is used to determine whether the fracture network can be produced (yes, if the in situ stress contrast is less than a given threshold value) in this region during the stimulation process. Guo et al. (2015) further investigated the interaction of the hydraulic and natural fractures for different in situ stress contrast cases. Their results demonstrated that at a stress contrast of 0 MPa, the propagation of the hydraulic fracture completely reopens natural fracture. When the stress contrast increased to 5 MPa, the natural fracture is partially opened by the hydraulic fracture. The opening and propagation of existing natural fractures will create a complex fracture network. The threshold value of in situ stress contrast for creating the fracture network is assumed to be 3 MPa in this paper. We use the threshold value to characterize the fracture network. The regions where in situ stress contrast is less than 3 MPa during fracture propagation represent a fracture network, as shown in Fig. 3. The main focus of this work is to investigate the high injection rate stimulation for decreasing stress anisotropy and improving the fracture complexity. It is reasonable to use this method to characterize the fracture network for the analysis. The simulation of complex fracture networks needs further work.

Fig. 4 demonstrates the variation of the fracture network during the fracturing process at the injection rate of 12 m^3/min. At the early stage of fracturing, the fracture network increases rapidly with the injection time due to the large fracture net pressure. After the injection time of 3 min is reached, the net pressure has nearly reached a threshold, and the fracture network area does not change for a longer injection time. The initiation and propagation of hydraulic fractures require high fluid pressure to overcome the tensile strength of the rock matrix. As fracture propagation, the leak-off rate (volume rate of fluid loss to the formation) increases due to the continuous enlarging fracture surfaces. The increasing fracture length and leak-off rate causes decreasing net pressure. Therefore, after some time of injection, the net pressure decreased to the threshold value, and the new fracture network cannot be created for further stimulation. This time depends on reservoir and fracturing fluid properties, such as in-situ stress, permeability, injection rate and fluid viscosity, etc. In addition, for multiple stages fracturing treatment, the mechanical interaction between fractures will affect the fractures net pressure as well as the critical injection time.

3.2.2 Effects of brittleness on fracture complexity

Brittleness is very important for the successful recovery of unconventional reservoirs, as discussed in the papers (Rickman et al., 2008; NcNeil et al., 2012; Rune et al., 2015; Zhang et al., 2016). Low brittle rocks have high porosity and low Young's modulus. The confining stress induced by hydraulic fracturing in ductile rocks will result in a large plastic deformation and the increase of Young's modulus in the

vicinity of the hydraulic fracture. There are the models introducing plasticity to represent brittleness (Haisham et al., 2011; Haisham and Rune, 2011). However, there is not much agreement on the exact definition of the rock brittleness in the scientific community, as many definitions can be found in a review paper (Zhang et al., 2016). The effect of brittleness on fracture networks is conducted by introducing a bulk modulus evolution model. The evolution of bulk modulus is shown in the following equation (Zimmerman, 1991).

$$\frac{1}{K}=\frac{1}{K^{\infty}}+\left(\frac{1}{K^{i}}-\frac{1}{K^{\infty}}\right)e^{-\sigma_e/p'} \tag{8}$$

where K^i and K^∞ refer to the bulk modulus at low and high effective pressures respectively. σ_e is the minimum effective in-situ stress. p' is characteristic closure pressure that depends on the solid and bulk properties. The increase of Young's modulus induced by confining stress is represented by the equation. Ductile rocks have a low K^i due to the large porosity. Three types of rocks are studied with the setting of K^i equal to 11MPa, 22MPa and 36MPa representing ductile, ductile-brittle and brittle rocks, respectively. The simulations are presented for single fracture with the injection rate of 10 m^3/min, and the other parameters are listed in Table 1. The variation of fracture network area with brittleness is shown in Fig.5.

It is shown that the fracture network area created in ductile rocks is very smaller than brittle rocks. The improvement percentage of fracture network area for brittle rocks is 214%. The brittleness plays a dominant role in the creation of the fracture network.

3.2.3 High injection rate stimulation in improving the fracture complexity

Five stimulation cases are simulated to investigate the effect of the injection rate on the fracture network area. The parameters listed in Table 1 are used. The injection rate ranges from 5 m^3/min to 15 m^3/min. The injection volume is 100 m^3 for every stimulation case. The fracture network area with varying injection rates is shown in Fig. 6. It is increased from approximately 100 m^2 to 200 m^2 in the single fracture stimulation. Consequently, a high injection rate stimulation can create a larger field of the fracture network. However, an extremely large injection rate stimulation requires special instruments in practical terms and may result in accidents. The simulated injection rate in this paper is set to be a wide range of practical engineering. The large fluid pressure within the fracture for high injection rate stimulation dramatically decreases the stress anisotropy in the vicinity of the fracture; therefore, a large field of the fracture network can be created.

3.2.4 Parameters effects

The effect of the injection rate on the fracture network for varying in situ stress fields is investigated. Three horizontal in situ stress cases, 50 MPa and 58 MPa, 50 MPa and 60 MPa and 55 MPa and 65 MPa are used. The injection rate is set as 5 m^3/min and 10 m^3/min for every in situ stress case. The other parameters listed in Table 1 are used. The fracture network area for varying in situ stresses and injection rates is shown in Fig. 7. For the first stress case (50 MPa and 58 MPa), the fracture network areas are 350 m^2 and 580 m^2 for the low and high injection rates, respectively.

The increment percentage of the fracture network area for a high injection rate is 65% in this case. For the second stress case (50 MPa and 60 MPa), the fracture network area is 104 m^2 and 160 m^2, respectively. The increment percentage of fracture network area for high injection rate in this case is 53%. It is known that the fracture network area decreases with initial in situ stress contrast. For the last stress case (50 MPa and 60 MPa), the fracture network areas are 250 m^2 and 350 m^2 for the low and high injection rates with an increment percentage of 40%. Increasing the confining stress promotes the growth of the fracture network. The hydraulic fracture is driven by high fluid pressure overcoming the confining stress and rock tensile strength to initiation and propagation. The fracture initiation process and the fracture aspect mainly depends on the initial minimum in situ stress. For the cases with the same minimum in situ stress and different stress contrast, the fracture network area is large for low stress contrast case. The confining stress prevents the fractures to propagate, which results in a large fracture aperture and in situ stress variations. Therefore, the fracture network area is large for high confining stresses condition.

We study the effect of permeability on the fracture network area. The injection rates are set to be 5 m^3/min and 10 m^3/min, respectively. The fracture network area with three permeabilities, 0.01 mD, 0.05 mD and 0.1 mD, is studied and the results are illustrated in Fig. 8. The fracture network area decreases with permeability. The increment percentages of the fracture network area for a high injection rate are 50%, 53% and 33%, respectively. The fracture network area increases significantly for low permeability cases. At a permeability of 0.1 mD, the fracture network area does not

show significant changes with different injection rates. Due to the small leak-off at low permeability reservoirs, the fracture width and net pressure is large with a significant effect on the in situ stress.

The brittleness of the rock matrix is significant for the successfully creation of the fracture network. Ductile rocks have a high porosity and low Young's modulus. The Young's modulus of porous rocks is not a constant in the field during fracture propagation. The evolution of bulk modulus is represented by equation 8. Three cases of Young's modulus, 20 GPa, 40 GPa and 60 GPa are studied, and the injection rates are set to be 5 m^3/min and 10 m^3/min, respectively. The fracture network area for varying Young's modulus and injection rates is demonstrated in Fig. 9. The fracture network area is increasing with Young's modulus. The propagation of hydraulic fracture in ductile rocks causes a large deformation of rock matrix in the vicinity of the fracture, while the deformation and stress perturbation in the far field of the fractures is small.

We further investigated the effect of Poisson's ratio on the fracture network area. The Poisson's ratios are set to be 0.1, 0.2 and 0.3, respectively. The injection rates are 5 m^3/min and 10 m^3/min for every Poisson's ratio case. Fig. 10 shows the fracture network area for different Poisson's ratios and injection rates. The fracture network area decreases slightly with Poisson's ratio. High injection rate stimulation improves the fracture network area for varying Poisson's ratio cases.

A tornado diagram is presented to show the relative importance of the parameters on the fracture network area for the high injection rate (Fig. 11). The figure

demonstrates the increment of the fracture network area for a high injection rate. The base value is based on the parameters listed in Table 1. It is shown that the in situ stress contrast, permeability and Young's modulus are the main parameters that influence the creation of fracture network.

Although the brittleness is very important for successfully creating fracture network as discussed above, it is a reservoir parameter and cannot be changed in the stimulation process. It can be used to predict whether a large field of fracture network can be created in a reservoir. For ductile-brittle or brittle rocks, adjusting the stimulation parameters such as injection rate is an effective method to improve fracture complexity. The discussion of high injection rate stimulation for improving fracture complexity is still meaningful.

3.3 Results of sequential multiple fractures treatments

Multi-fracture treatments in horizontal wells comprise the key technology that economically depletes unconventional gas or oil reservoirs. The simulation of sequential fracturing for four fractures is performed. The injection rate is 10 m^3/min with a duration of 30 min for a single fracture. The fracture spacing is 50 m. The formation permeability is 0.5 mD. The other parameters are shown in Table 1. The simulation results are demonstrated in Fig. 12. The first fracture propagates perpendicular to the horizontal well as shown in Fig. 12 (a). After the first fracture is stimulated, the distributed truss elements on the fracture surface are active,

characterizing the injected proppant to prevent fracture closure. The second fracture tends to grow away from the first one to some extent due to the stress perturbation induced by the propped fracture (Fig. 12b), and this tendency reduces the negative mechanical interaction between fractures. The regions of the fracture network produced at the second stage (Fig. 12b) in the vicinity of the second fracture are larger than the first one (Fig. 12a) because of the stress interaction between fractures. The regions of the fracture network are further increased after the third fracture stimulated as illustrated in Fig. 12 (c). Furthermore, the fourth fracture creates a larger fracture network than previous fractures (Fig. 12d). The mechanical interaction of multiple-fracture treatments in horizontal wells decreases the in situ stress anisotropy and the large field of the fracture network can be created. The fracture network created by sequential multiple fracture treatments in horizontal wells is larger than the same numbers of single fractures.

The study of the effect of the injection rate on the fracture network for multiple fracture treatments in horizontal wells is performed. We simulated eight fractures with the sequential injection method. The fracture spacings are 50 m and 70 m, respectively. The injection rates are 5 m^3/min and 10 m^3/min for every fracture spacing case. The fracture network for varying fracture spacings and injection rates is shown in Fig. 13. The average fracture network width (AFNW) is used in this paper. It is defined as the fracture network area between fractures / fracture spacing after fracturing. It can be used to characterize the regions of the fracture network at different fracture spacings. The evolution of AFNW for varying spacings and injection rates is demonstrated in

Fig. 14. The AFNW increases with each additional fracture in the four cases. After the first fracture is stimulated, the AFNW corresponding to the injection rates of 5 m^3/min and 10 m^3/min shows the differences that are the same with single fracture treatments presented above. As the number of fracturing stages increases, the curves for the injection rates of 5 m^3/min and 10 m^3/min diverge, showing the increasing mechanical interaction between fractures with a high injection rate stimulation in the horizontal well. The high injection rate stimulation method significantly improves the AFNW at different fracture spacings (50 m and 70 m). In addition, the increment of the fracture interaction of multiple fractures in decreasing stress anisotropy is further accentuated by the high injection rate stimulation; therefore, a larger field of fracture network can be created.

3.4 Results of simultaneous fracturing treatment

The simulation of simultaneous fracturing for two fractures is performed. The fracture spacing is set to be 40 m and 60 m, respectively. The injection rates are 5 m^3/min and 10 m^3/min for every fracture spacing case. The injection volume is 500 m^3. The formation permeability is 0.1 mD. The other parameters are listed in Table 1. Fig. 15 shows the fracture network for varying injection rates and fracture spacings. The fracture network produced by high injection rate for different fracture spacings is larger than the low injection rate cases.

4. Conclusion

The variation in the in situ stress as well as the fracture network during the

fracturing process is investigated by a fully coupled hydro-mechanical propagation model based on XFEM. Single fracture analysis shows that the opened hydraulic fracture decreases in situ stress contrast in its neighborhood and the stress contrast along horizontal well increases with the injection time. The fracture network area increases linearly with the injection rate. Sensitivity studies of the single fracture demonstrated that a high injection rate treatment improves the fracture network area at different in situ stress cases. At relatively low stress contrast formations, the large field of the fracture network area could be created by the high injection rate stimulation method. In addition, the fracture network area significantly increases for the condition of low permeability reservoirs. The fracture network area increases with Young's modulus.

The decrease in the in situ stress anisotropy is accentuated when sequential multiple fracture treatments in the horizontal well are implemented due to the mechanical interaction between fractures. The created fracture network area increases significantly with the number of fractures, indicating the increased mechanical interaction between fractures. The stress interaction of multiple fractures in decreasing stress anisotropy is further accentuated by the high injection rate stimulation method, and larger field fracture networks can be created. If the formation in situ stress contrast or permeability is large, a large field of fracture network cannot be created for single fracture treatment. Sequential multiple fractures treatments with a high injection rate stimulation method must be implemented to decrease the stress anisotropy and improve the fracture complexity. The simulation of simultaneous

fracturing demonstrated that the fracture network produced by a high injection rate treatment is larger than the low injection rate cases.

High injection rate stimulation must be implemented using special instruments due to the increase of injection pressure. The stimulation method has been successfully used in a Chinese oilfield and acquires a good result. The limitation for increasing the rate of injection is the increasing of surface pressure, which may result in accidents. The optimal injection rate depends on the instruments, reservoir parameters and the cost, etc. The main focus of this work is to investigate the high injection rate stimulation for decreasing stress anisotropy and improving the fracture complexity in single and multiple stages fracturing treatments. The cost is not considered in this work. The optimal injection rate is determined by the upper limit of the surface pressure. A comprehensive study of optimal injection rate stimulation combining more factors needs to be further work.

The results of this work can be used in the hydraulic fracturing design to decrease the in situ stress anisotropy and improve the fracture complexity. Numerical simulation of fracture network in porous media remains challenging. The combination of natural fracture opening, intersection and fluid leak-off inside the natural fractures in porous media in this model requires further work.

Table 1 Input parameters for simulation cases

Input parameters	Value	Units
Young's modulus	50	GPa
Poisson's ratio	0.2	
Fluid viscosity	10	mPa · s
Tensile strength	2	MPa
Formation permeability	0.05	mD
Fracture height	80	m
Initial fracture half-length	1	m
Initial pore pressure	40	MPa
Maximum in situ horizontal stress	60	MPa
Minimum in situ horizontal stress	50	MPa
Porosity	0.08	

Acknowledgments

This work was jointly supported by National Natural Science Foundation of China (11472263, 11525211).

References

Alassi H, Holt R, 2011. Modeling Fracturing in Rock using a Modified Discrete Element Method with Plasticity. Key Engineering Materials, Trans Tech Publications. 452: 861-864.

Alassi, H. T., Holt, R. M., Nes, O. M., and Pradhan, S., 2011. Realistic geomechanical modeling of hydraulic fracturing in fractured reservoir rock. SPE paper 149375-MS. In: Canadian Unconventional Resources Conference, 15-17 November, Calgary, Alberta, Canada.

Batchelor, G.K., 1967. An introduction to fluid dynamics. Cambridge university press.

Belytschko, T. and Black, T., 1999. Elastic crack growth in finite elements with minimal remeshing. International journal for numerical methods in engineering. 45(5): 601-620.

Chen, Z., 2012. Finite element modelling of viscosity-dominated hydraulic fractures. Journal of Petroleum Science and Engineering. 88: 136-144.

Dahi-Taleghani, A. and Olson, J.E., 2011. Numerical modeling of multistranded-hydraulic-fracture propagation: Accounting for the interaction between induced and natural fractures. SPE journal. 16(03): 575-581.

Dontsov, E. and Peirce, A., 2014. Slurry flow, gravitational settling and a proppant transport model for hydraulic fractures. Journal of Fluid Mechanics. 760: 567-590.

Dontsov, E. and Peirce, A., 2015. Proppant transport in hydraulic fracturing: Crack tip

screen-out in KGD and P3D models. International Journal of Solids and Structures. 63: 206-218.

Fu, P., Johnson, S.M. and Carrigan, C.R., 2013. An explicitly coupled hydro‐geomechanical model for simulating hydraulic fracturing in arbitrary discrete fracture networks. International Journal for Numerical and Analytical Methods in Geomechanics. 37(14): 2278-2300.

Guo, J., Lu, Q., Zhu, H., Wang, Y. and Ma, L., 2015a. Perforating cluster space optimization method of horizontal well multi-stage fracturing in extremely thick unconventional gas reservoir. Journal of Natural Gas Science and Engineering. 26: 1648-1662.

Guo, J., Zhao, X., Zhu, H., Zhang, X. and Pan, R., 2015b. Numerical simulation of interaction of hydraulic fracture and natural fracture based on the cohesive zone finite element method. Journal of Natural Gas Science and Engineering. 25: 180-188.

Haifeng, Z. et al., 2013. New insight into mechanisms of fracture network generation in shale gas reservoir. Journal of Petroleum Science and Engineering. 110: 193-198.

Holt, R. M., Fjær, E., Stenebråten, J. F., and Nes, O. M., 2015. Brittleness of shales: Relevance to borehole collapse and hydraulic fracturing. Journal of Petroleum Science and Engineering. 131, 200-209.

Rickman, R., Mullen, M. J., Petre, J. E., Grieser, W. V., and Kundert, D., 2008. A practical use of shale petrophysics for stimulation design optimization: All

shale plays are not clones of the Barnett Shale. SPE paper 115258-MS, In: SPE Annual Technical Conference and Exhibition, 21-24 September, Denver, Colorado, USA.

Kresse, O., Weng, X., Gu, H. and Wu, R., 2013. Numerical modeling of hydraulic fractures interaction in complex naturally fractured formations. Rock mechanics and rock engineering. 46(3): 555-568.

Liu, C., Liu, H., Zhang, Y., Deng, D. and Wu, H., 2015. Optimal spacing of Staged fracturing in Horizontal shale-gas well. Journal of Petroleum Science and Engineering. 132: 86-93.

Liu, C. et al., 2016. Optimal spacing of sequential and simultaneous fracturing in horizontal well. Journal of Natural Gas Science and Engineering. 29: 329-336.

Marino, M.A. and Luthin, J.N., 1982. Seepage and groundwater. Elsevier.

Melenk, J.M. and Babuška, I., 1996. The partition of unity finite element method: basic theory and applications. Computer methods in applied mechanics and engineering. 139(1): 289-314.

Mohammadnejad, T. and Andrade, J., 2016. Numerical modeling of hydraulic fracture propagation, closure and reopening using XFEM with application to in‐situ stress estimation. International Journal for Numerical and Analytical Methods in Geomechanics. 40(15): 2033-2060.

Mohammadnejad, T. and Khoei, A., 2013a. An extended finite element method for hydraulic fracture propagation in deformable porous media with the cohesive crack model. Finite Elements in Analysis and Design. 73: 77-95.

Mohammadnejad, T. and Khoei, A., 2013b. Hydro‐mechanical modeling of cohesive crack propagation in multiphase porous media using the extended finite element method. International Journal for Numerical and Analytical Methods in Geomechanics. 37(10): 1247-1279.

Morrill, J. and Miskimins, J.L., 2012. Optimization of hydraulic fracture spacing in unconventional shales. SPE paper 152595-MS. In: SPE Hydraulic Fracturing Technology Conference, 6-8 February, The Woodlands, Texas, USA.

McNeil, F., Van Gijtenbeek, K., and Van Domelen, M., 2012. New hydraulic fracturing process enables far-field diversion in unconventional reservoirs, SPE paper SPE-152704-MS. In: SPE/EAGE European Unconventional Resources Conference and Exhibition, 20-22 March, Vienna, Austria.

November, Denver, Colorado, USA Olson, J.E. and Taleghani, A.D., 2009. Modeling simultaneous growth of multiple hydraulic fractures and their interaction with natural fractures, SPE paper 119739-MS. In: SPE Hydraulic Fracturing Technology Conference, 19-21 January, The Woodlands, Texas.

Riahi, A. and Damjanac, B., 2013. Numerical study of interaction between hydraulic fracture and discrete fracture network. In: International Conference for Effective and Sustainable Hydraulic Fracturing, Brisbane, Australia, 20–22 May.

Roussel, N.P. and Sharma, M.M., 2011a. Optimizing fracture spacing and sequencing in horizontal-well fracturing. SPE Production & Operations. 26(02): 173-184.

Roussel, N.P. and Sharma, M.M., 2011b. Strategies to minimize frac spacing and

stimulate natural fractures in horizontal completions, SPE paper 146104-MS. In: SPE Annual Technical Conference and Exhibition, 30 October-2 November, Denver, Colorado, USA.

Shi, F., Wang, X., Liu, C., Liu, H. and Wu, H., 2016. A coupled extended finite element approach for modeling hydraulic fracturing in consideration of proppant. Journal of Natural Gas Science and Engineering. 33: 885-897.

Sneddon, I.N., 1946. The distribution of stress in the neighbourhood of a crack in an elastic solid. Proc. R. Soc. Lond. Ser. A. Math. Phys. Sci. 187 (1009), 229–260.

Soliman, M.Y., East, L.E. and Augustine, J.R., 2010. Fracturing design aimed at enhancing fracture complexity, SPE paper 130043-MS. In: SPE EUROPEC/EAGE Annual Conference and Exhibition, 14-17 June, Barcelona, Spain.

Wang, H., 2015. Numerical modeling of non-planar hydraulic fracture propagation in brittle and ductile rocks using XFEM with cohesive zone method. Journal of Petroleum Science and Engineering. 135: 127-140.

Wang, H., Liu, H., Wu, H. and Wang, X., 2015. A 3D numerical model for studying the effect of interface shear failure on hydraulic fracture height containment. Journal of Petroleum Science and Engineering. 133: 280-284.

Wang, X., Liu, C., Wang, H., Liu, H. and Wu, H., 2016. Comparison of consecutive and alternate hydraulic fracturing in horizontal wells using XFEM-based cohesive zone method. Journal of Petroleum Science and Engineering. 143:

14-25.

Weng, X., 2015. Modeling of complex hydraulic fractures in naturally fractured formation. Journal of Unconventional Oil and Gas Resources. 9: 114-135.

Zhang, X. and Jeffrey, R.G., 2014. Role of overpressurized fluid and fluid-driven fractures in forming fracture networks. Journal of Geochemical Exploration. 144: 194-207.

Zhou, L., Hou, M.Z., Gou, Y. and Li, M., 2014. Numerical investigation of a low-efficient hydraulic fracturing operation in a tight gas reservoir in the North German Basin. Journal of Petroleum Science and Engineering. 120: 119-129.

Zhang, D., Ranjith, P. G., and Perera, M. S. A., 2016. The brittleness indices used in rock mechanics and their application in shale hydraulic fracturing: A review. Journal of Petroleum Science and Engineering. 143, 158-170.

Zimmerman, R.W., 1990. Compressibility of Sandstones. Elsevier.

Captions of figures

Fig. 1. Schematic representation of fluid flow patterns in a fracture.

Fig.2. Comparison between simulated and field measured surface pressure curves.

Fig. 3. Variation of in situ stress contrast along the horizontal well, starting from the center of the fracture.

Fig. 4. Fracture network area with a varying injection time; the red regions represent the fracture network

Fig.5. The effect of brittleness on fracture network area

Fig. 6. Fracture network area with varying injection rates

Fig. 7. Fracture network area versus in situ stress for varying injection rates

Fig. 8. Fracture network area versus permeability for varying injection rates

Fig. 9. Fracture network area versus Young's modulus for varying injection rates

Fig. 10. Fracture network area versus Poisson's ratio for varying injection rates

Fig. 11. Tornado diagram for high injection rate stimulation

Fig. 12. Illustration of the fracture trajectory and network at different fracturing stages; the injection sequence is from right to left.

Fig. 13. Fracture network with different fracture spacings and injection rates. (a) Fracture spacing=50 m and injection rate=5 m^3/min, (b) fracture spacing=50 m and injection rate=10 m^3/min, (c) fracture spacing=70 m and injection rate=5 m^3/min and (d) fracture spacing=70 m and injection rate=10 m^3/min.

Fig. 14. Evolution of the AFNW with each additional consecutive fracture with different fracture spacings and injection rates

Fig. 15. Fracture network with different fracture spacings and injection rates. (a) Fracture spacing=40 m and injection rate=5 m^3/min, (b) fracture spacing=40 m and injection rate=10 m^3/min, (c) fracture spacing=60 m and injection rate=5 m^3/min, and (d) fracture spacing=60 m and injection rate=10 m^3/min.

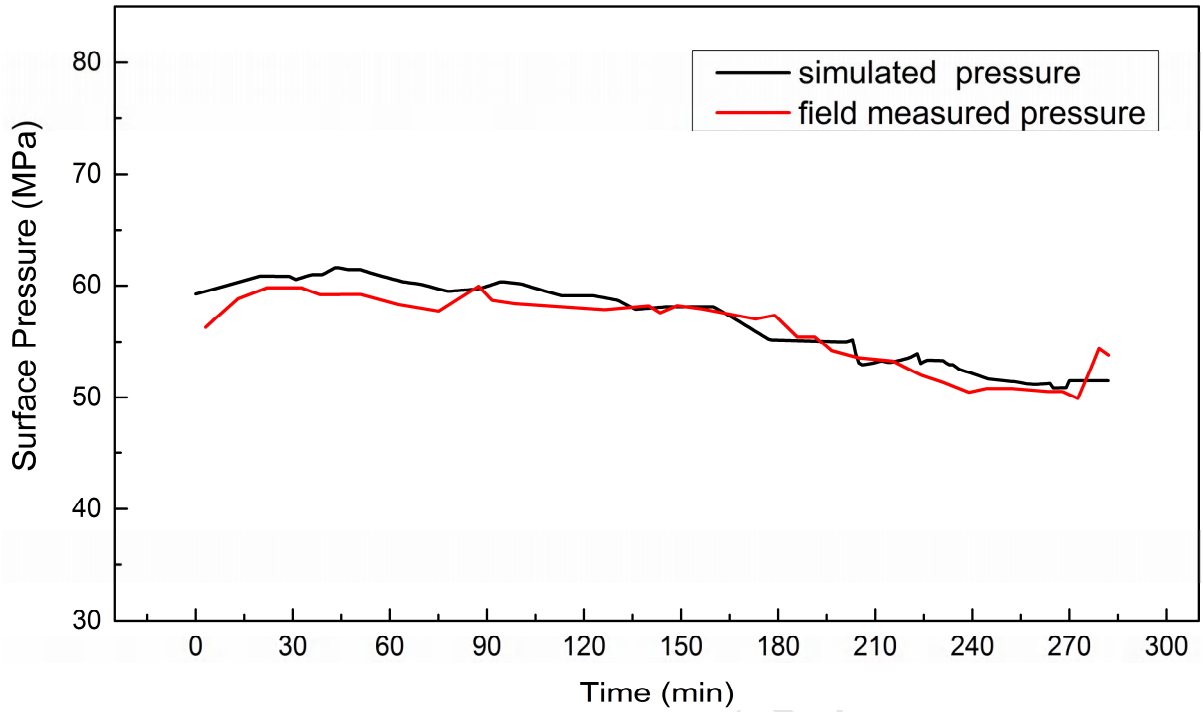

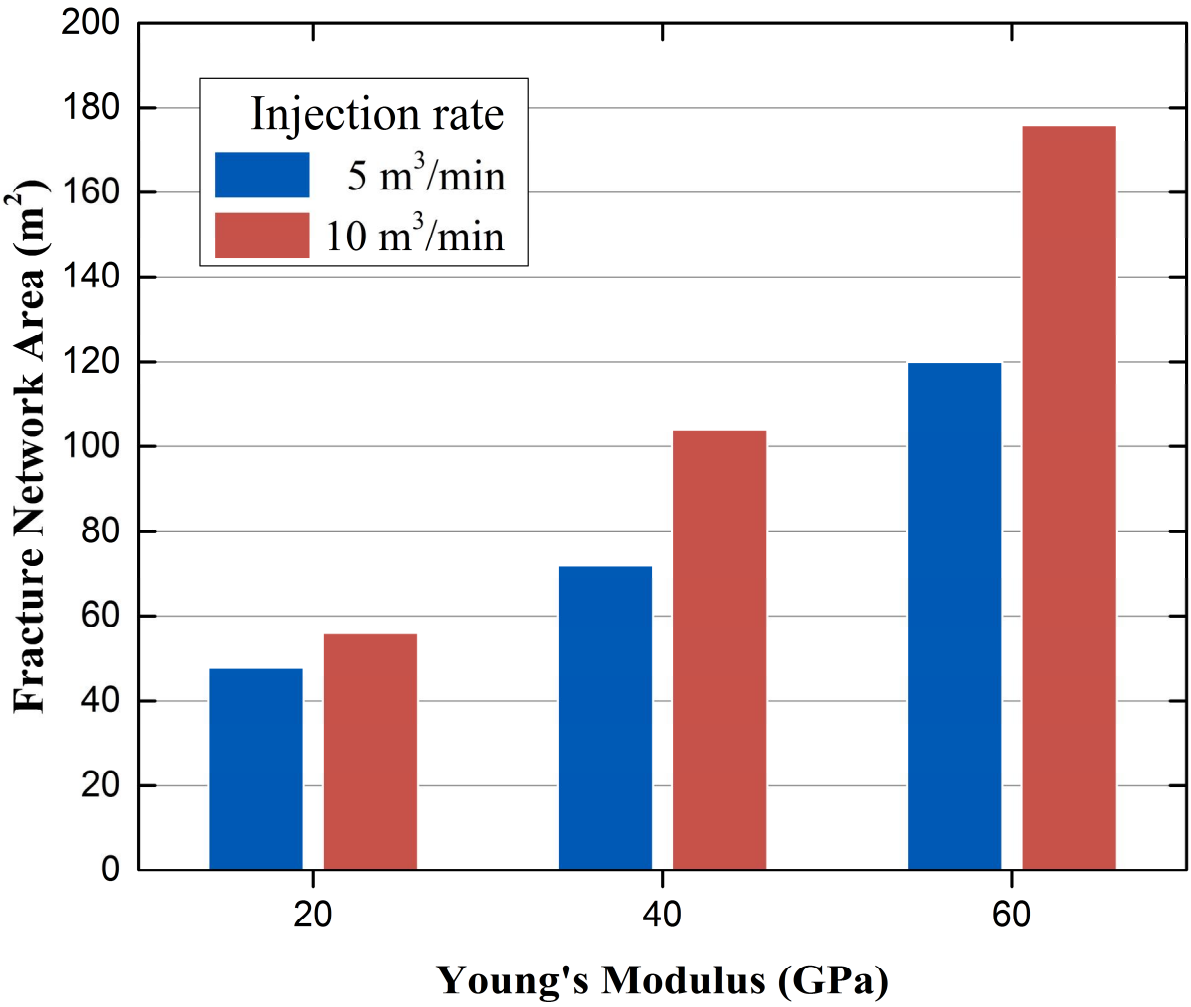
Injection rate
5 m3/min
10 m3/min
Fracture Network Area (m2)
Young's Modulus (GPa)
0
20
40
60
80
100
120
140
160
180
200
20
40
60

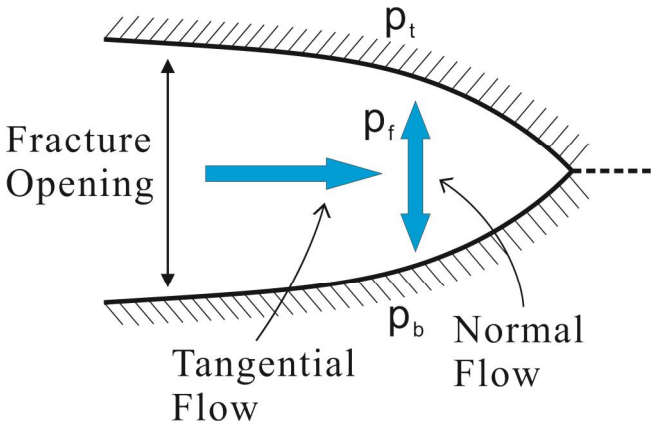

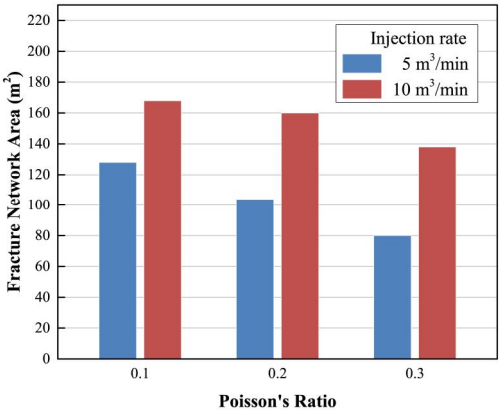

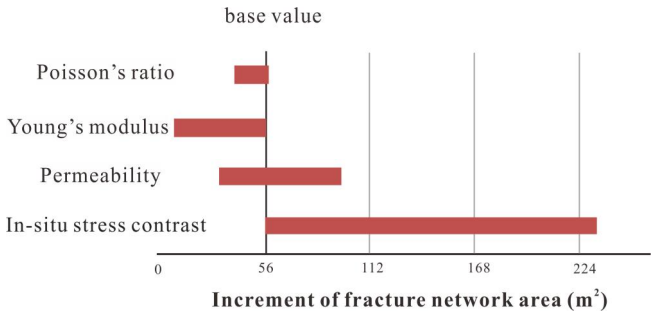

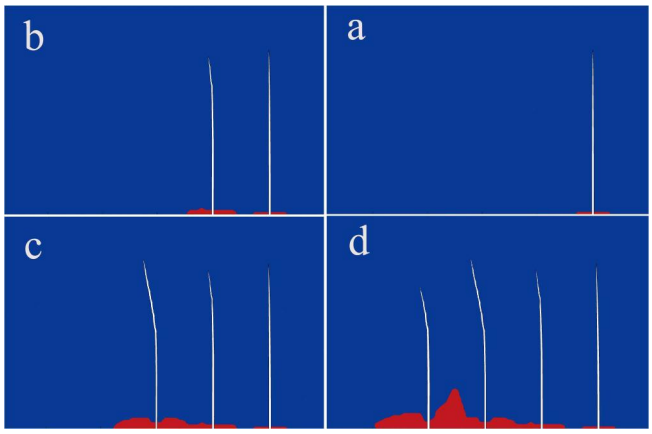

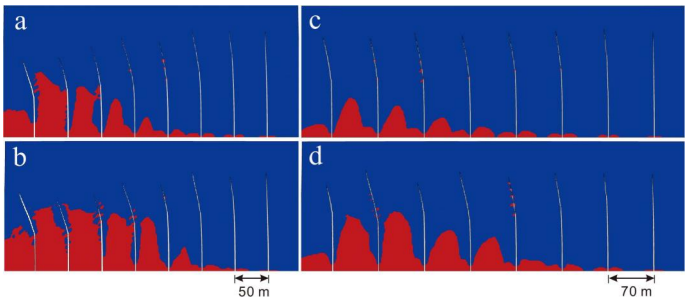

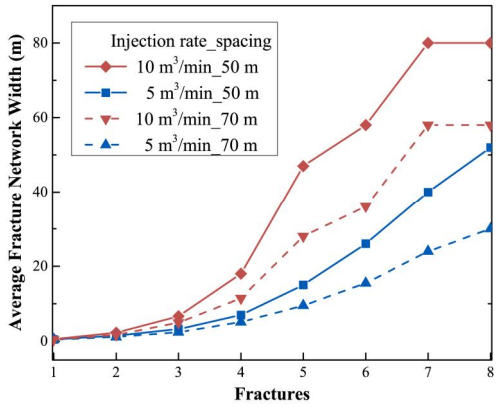

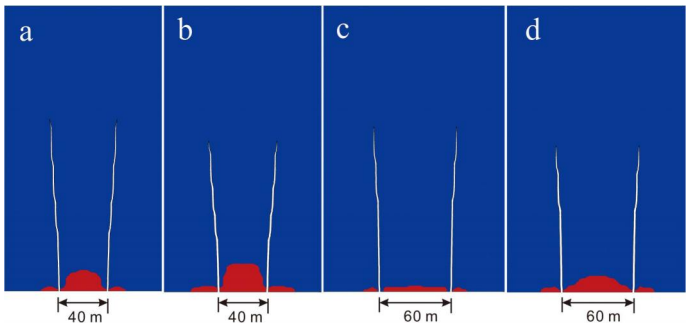

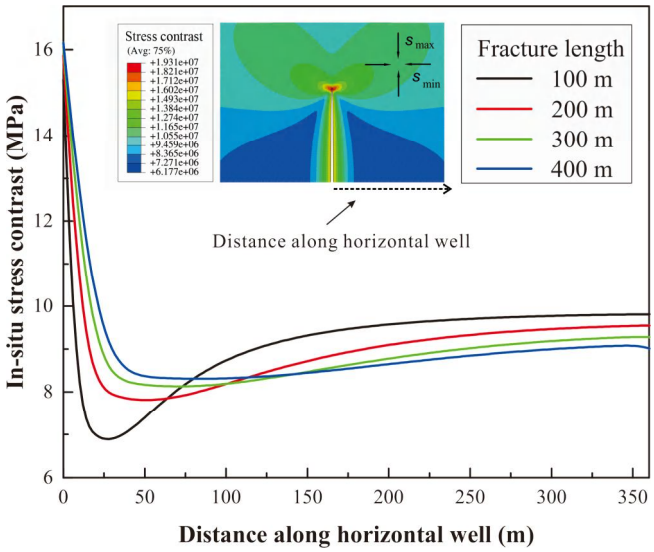

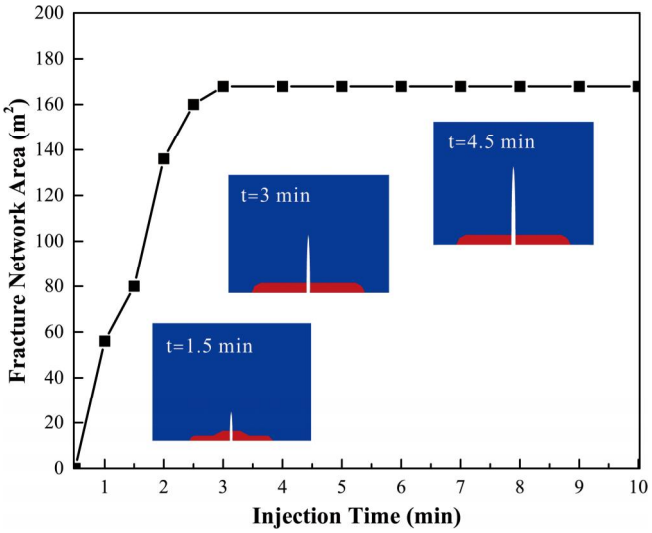

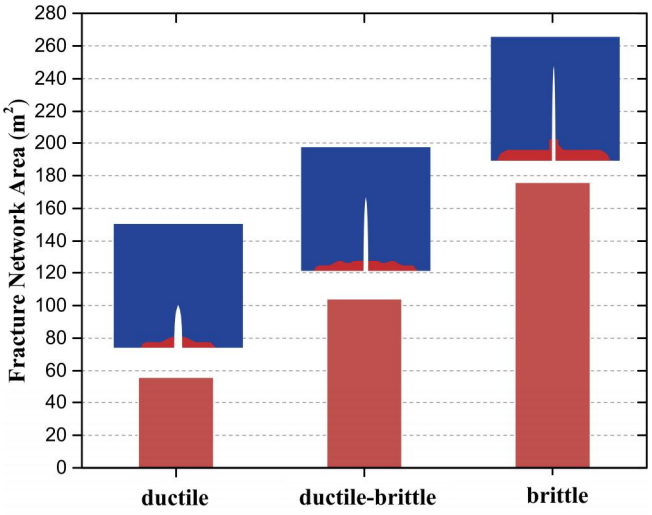

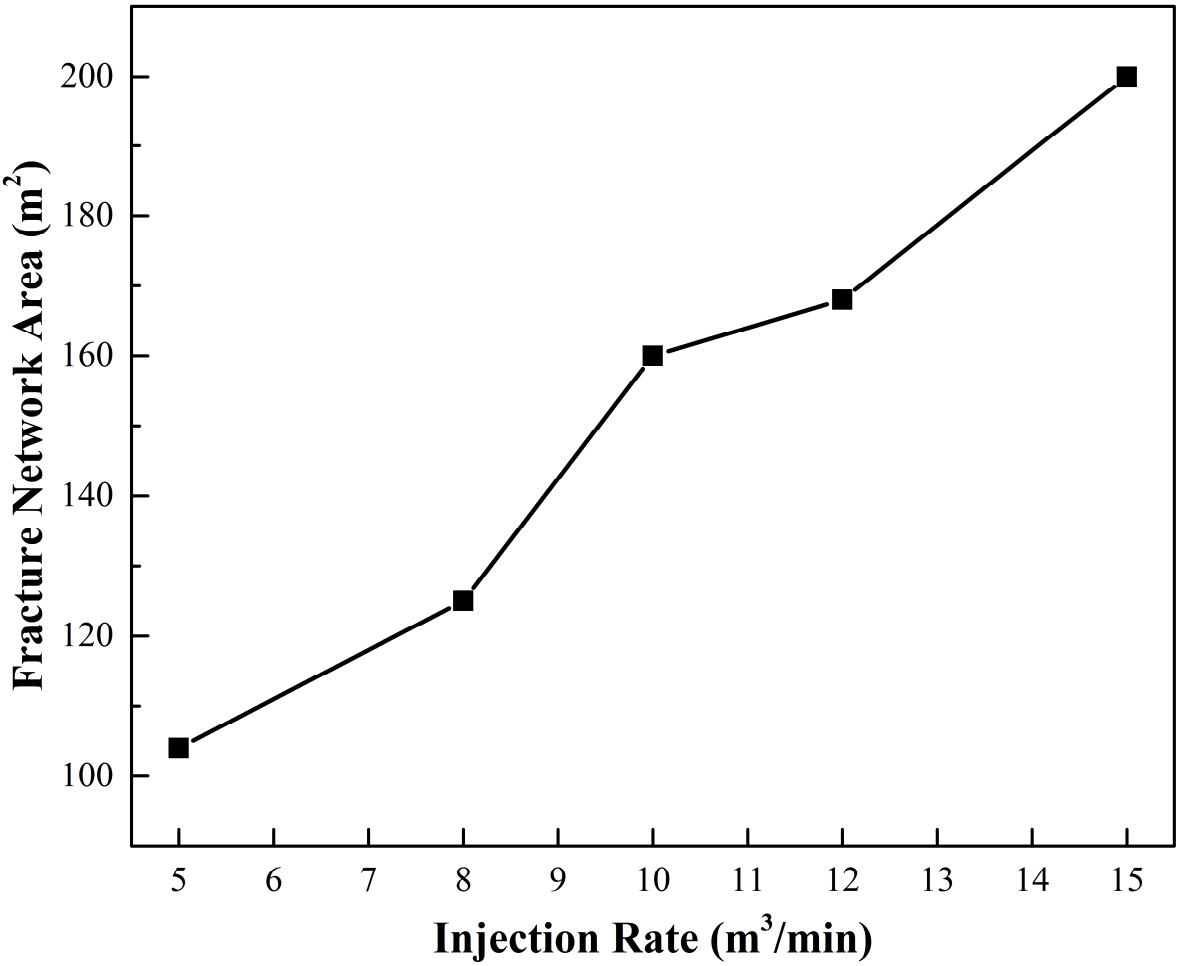
Fracture Network Area (m²)
200
180
160
140
120
100
5
6
7
8
9
10
11
12
13
14
15
Injection Rate (m³/min)

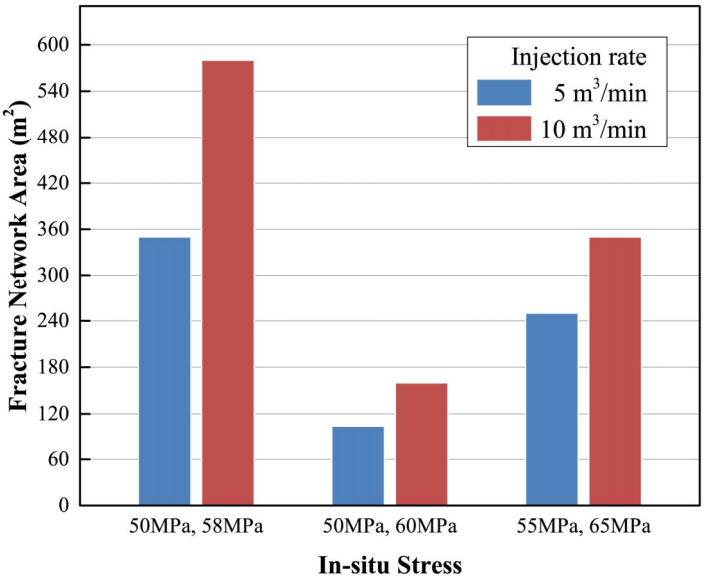

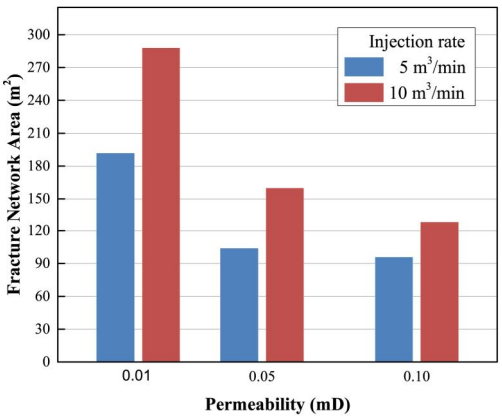

Highlights

- The variations of in-situ stress and fracture network during nonplanar fractures propagation are simulated.
- How to decrease stress anisotropy and improving fracture complexity in unconventional reservoirs is presented.
- In-situ stress contrast, permeability and Young's modulus play a significant role in hydraulic fracturing design.